

Table 1. GRNs built in this study.

Network type	Study	Note	N	Network label
Tissue	Stelpflug et al. 2016	B73	93	Stelpflug2016 B73 [93]
	Walley et al. 2016	B73	23	Walley2016 B73 [23]
	Zhou et al. 2018	B73	23	Zhou2018 B73 [23]
		Mo17	23	Zhou2018 Mo17 [23]
	Yi et al. 2019	BxM	23	Zhou2018 BxM [23]
		seed dev	31	Yi2019 seed dev [31]
	Tissue Atlas	combined	247	Tissue Atlas combined [247]
Genotype	Eichten et al. 2013	seedling_leaf3	62	Eichten2013 seedling_leaf3 [62]
	Fu et al. 2013	kernel	368	Fu2013 kernel [368]
	Hirsch et al. 2014	seedling	503	Hirsch2014 seedling [503]
	Leiboff et al. 2015	SAM	383	Leiboff2015 SAM [383]
	Lin et al. 2017	ear	26	Lin2017 ear [26]
		root	27	Lin2017 root [27]
		shoot	27	Lin2017 shoot [27]
		tassel	26	Lin2017 tassel [26]
		SAM	27	Lin2017 SAM [27]
	Kremling et al. 2018	GRoot	201	Kremling2018 GRoot [201]
		GShoot	271	Kremling2018 GShoot [271]
		Kern	226	Kremling2018 Kern [226]
		L3Base	254	Kremling2018 L3Base [254]
		L3Tip	257	Kremling2018 L3Tip [257]
		LMAD	199	Kremling2018 LMAD [199]
	Shaefer et al. 2018	LMAN	249	Kremling2018 LMAN [249]
		root_GCN	48	Shaefer2018 root_GCN [48]
	Huang et al. 2018	leaf	394	Huang2018 leaf [394]
		root	176	Huang2018 root [176]
		SAM	406	Huang2018 SAM [406]
		seed	159	Huang2018 seed [159]
	Mazaheri et al. 2019	seedling	453	Mazaheri2019 seedling [453]
	Li et al. 2019	endosperm	121	Li2019 endosperm [121]
		internode	77	Li2019 internode [77]
		leaf	84	Li2019 leaf [84]
		root	84	Li2019 root [84]
		shoot	85	Li2019 shoot [85]
		seedling	169	Li2019 seedling [169]
Tissue*Genotype	Lin et al. 2017	5 tissues	133	Lin2017 5 tissues [133]
	Kremling et al. 2018	7 tissues	1,657	Kremling2018 7 tissues [1657]
	Huang et al. 2018	4 tissues	1,136	Huang2018 4 tissues [1136]
	Zhou et al. 2018	B+M+F1	73	Zhou2018 B+M+F1 [73]
	Li et al. 2019	6 tissues	620	Li2019 6 tissues [620]
RIL	Li et al. 2013	B73 x Mo17	107	Li2013 B73 x Mo17 [107]
	Baute et al. 2016	MAGIC	102	Baute2016 MAGIC [102]
	Baute et al. 2015	B73 x H99	106	Baute2015 B73 x H99 [106]
	Wang et al. 2018	W22 x Teosinte	617	Wang2018 W22 x Teosinte [617]

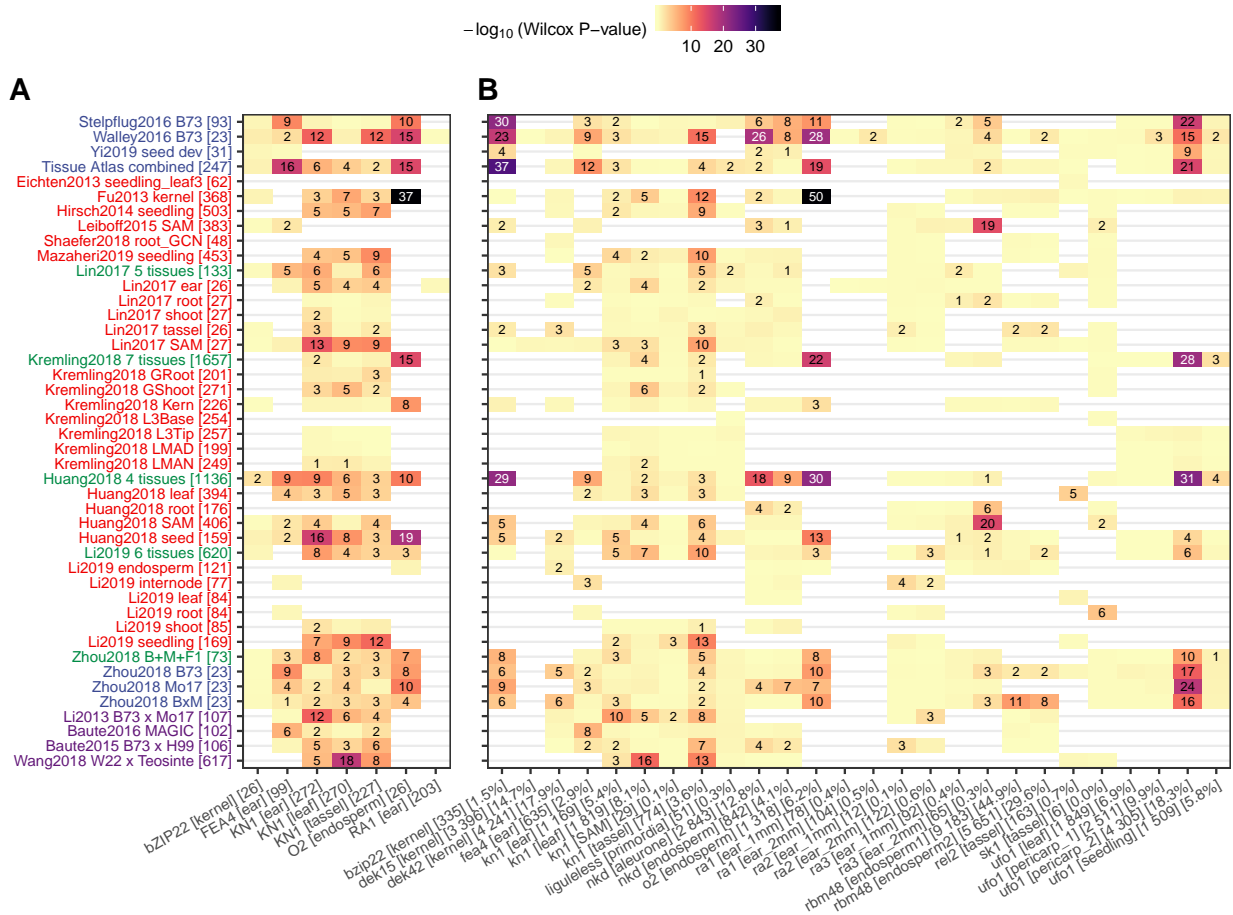


Figure 1. TF-target interactions predicted by GRNs are supported by knockout mutant RNA-Seq experiments. (A) direct targets of published TF studies; (B) For each one of the 21 maize TFs with knockout mutant RNA-Seq data available, differentially expressed genes between mutant and wildtype were identified using DESeq2 ($p\text{-value} < 0.01$). Wilcox rank test were then performed using the predicted (TF-target) interaction scores between the group of true targets (DEGs) and non-targets (non-DEGs). Numbers in each cell show the actual test P-value ($-\log_{10}$ transformed) with blank cells standing for “not significant” ($P > 0.05$). White cells stand for missing data where the TF being tested (knocked out) is not expressed in the corresponding GRN. Y-axis labels correspond to the different networks listed in Table 1. X-axis labels show the common name for each TF, the tissue in which the TF is expressed, number of direct targets (Panel A) or number and proportion of differentially expressed genes in TF mutant (Panel B) as listed in Table S1.

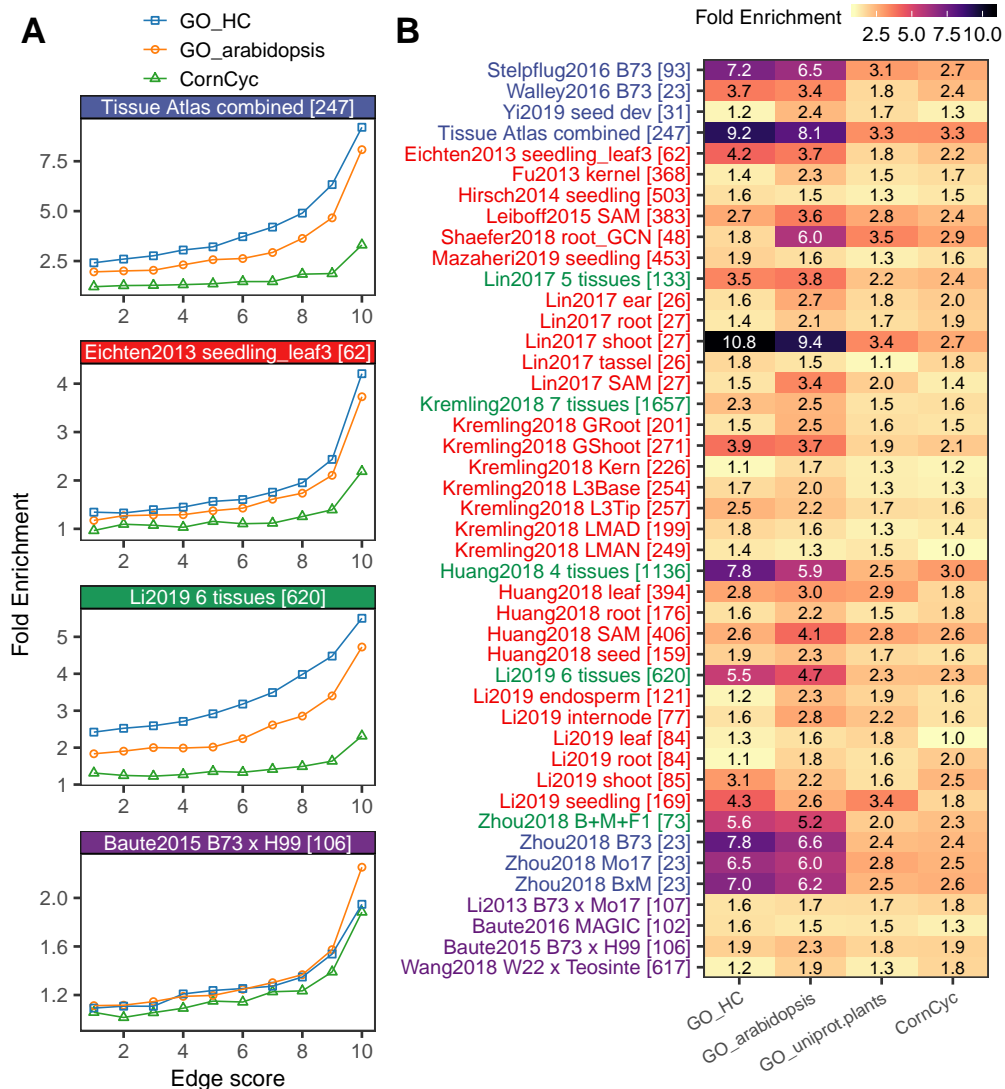


Figure 2. Enrichment of co-annotated GO/CornCyc terms in co-regulated network targets. For each network the top 1 million predicted TF-target associations were binned to 10 bins and assessed for enrichment of GO/CornCyc functional annotation. Fold enrichment is calculated as the observed number of shared GO/CornCyc terms (by targets regulated by a common TF) divided by the expected number of shared annotation terms (determined by permutation). (A) GO/CornCyc enrichment is shown for 4 selected networks. (B) Heatmap showing enrichment of co-annotated GO/CornCyc terms in the first bin (i.e., top 100k) of edges in the GRNs. See Figure S7 for the enrichment in all bins of all built GRNs. A total of six sources of GO annotation were used but only three were shown here: GO_HC (high quality hand-curated terms transferred from maize AGP_v3 annotation), GO_arabidopsis and GO_uniprot.plants (check Figure S7 for a complete list)

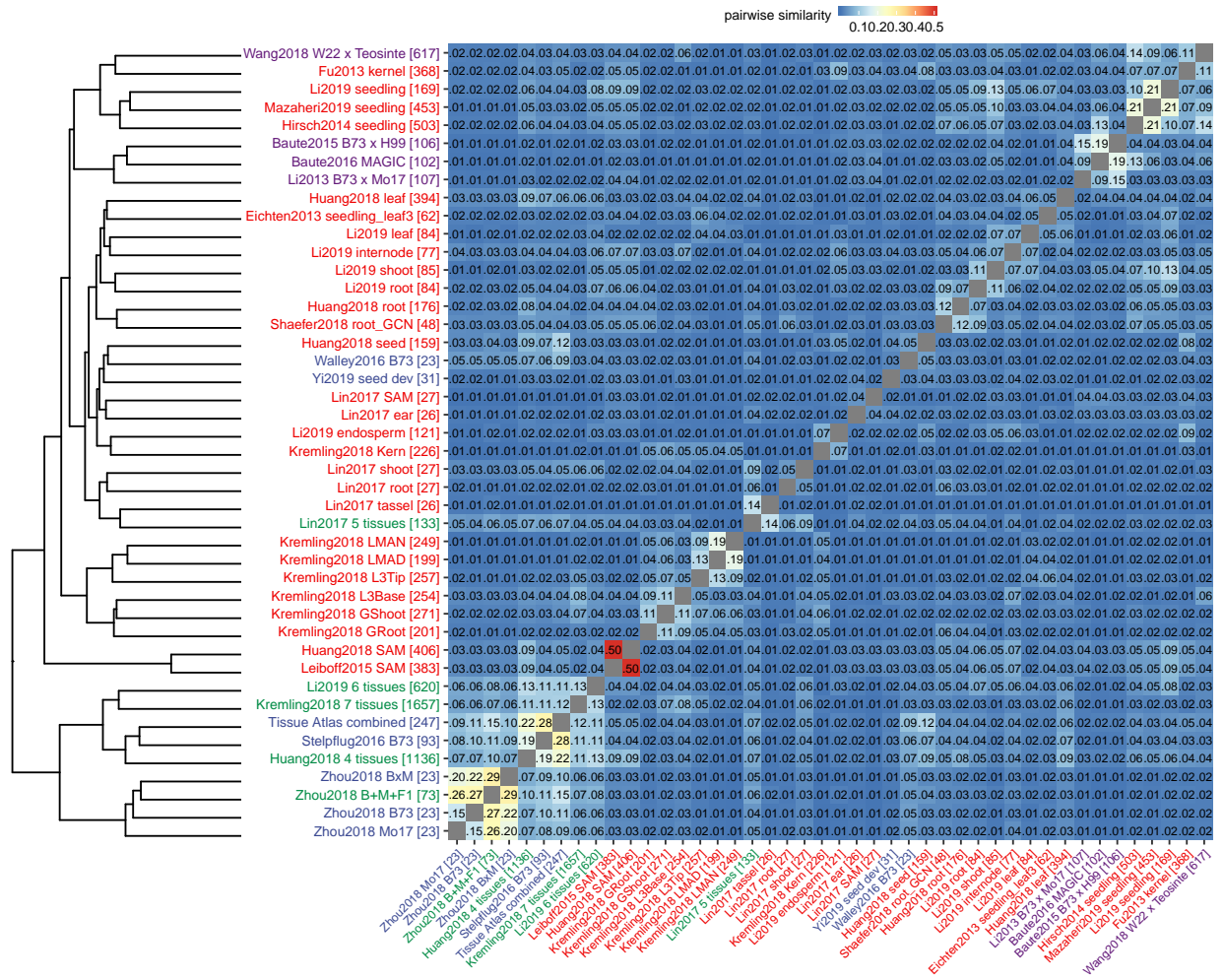


Figure 3. Hierarchical clustering of 44 GRNs. Pairwise distance between networks was determined by taking the top 100,000 TF-target predictions from each network and calculating the proportion of shared (common) predictions (using ‘dist()’ function in R with additional argument ‘method=binary’). Hierarchical clustering was then performed based on the cross-network pairwise distance matrix using “ward.D” method.

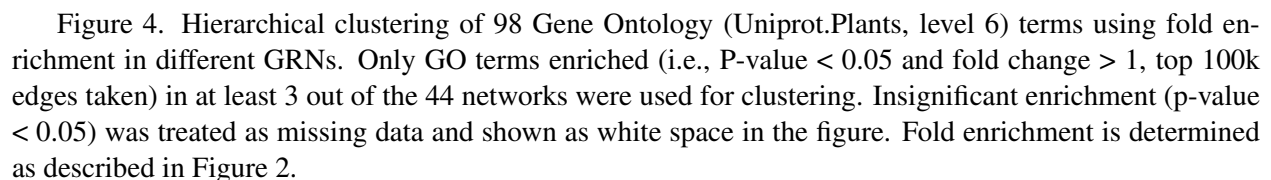


Figure 4. Hierarchical clustering of 98 Gene Ontology (Uniprot.Plants, level 6) terms using fold enrichment in different GRNs. Only GO terms enriched (i.e., P-value < 0.05 and fold change > 1 , top 100k edges taken) in at least 3 out of the 44 networks were used for clustering. Insignificant enrichment (p-value < 0.05) was treated as missing data and shown as white space in the figure. Fold enrichment is determined as described in Figure 2.

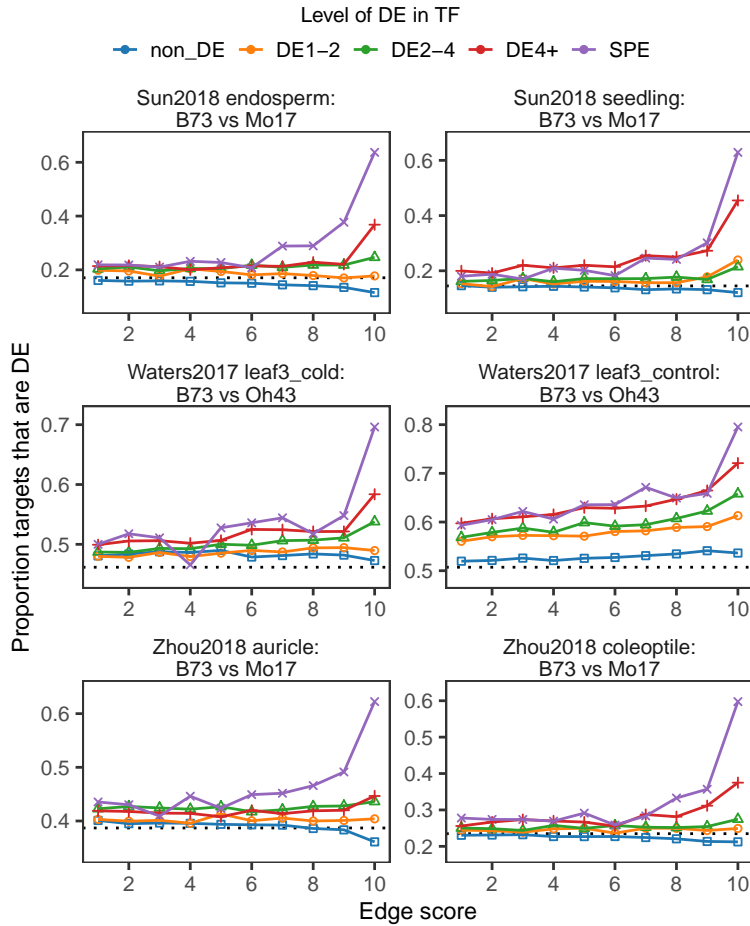


Figure 5. TF-target validation of the combined tissue network in three selected natural variation datasets. Each panel shows the proportion of differentially expressed targets regulated by TFs showing different DE levels between two genotypes in one tissue/treatment condition. For each network the top 1 million TF-target predictions were binned to 10 groups based on the interaction score in GRN. Each TF-target pair is classified according to the DE level of the TF (“non_DE”, “DE1-2”, “DE2-4”, “DE4+” or “SPE”) in each network. The proportion of TF-target pairs with the target also showing DE was then determined for each category. Dashed line in each panel represents the genome-wide (background) proportion of DE genes in each tissue/treatment setting.

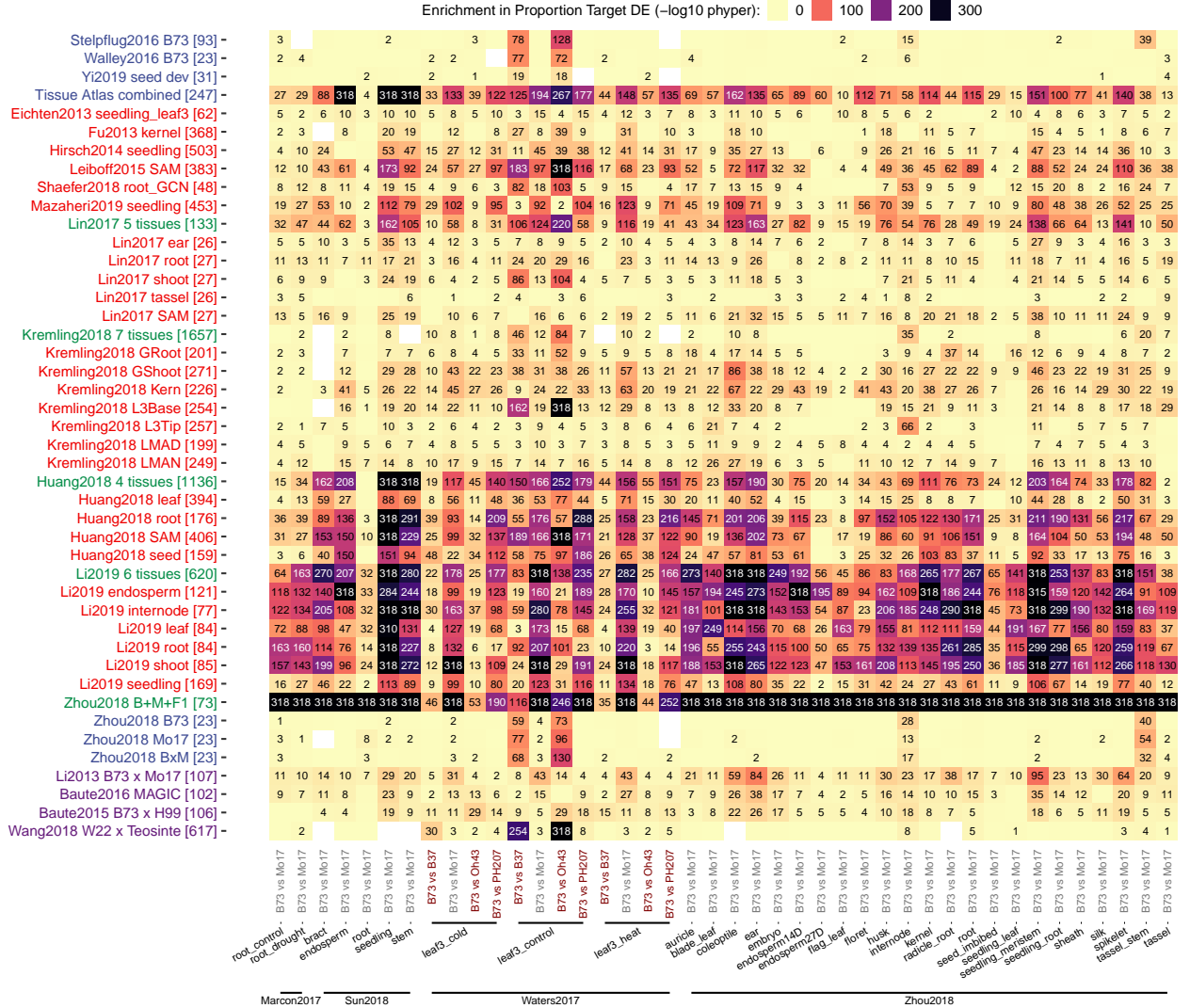


Figure 6. Enrichment in differentially expressed targets regulated by TFs that show SPE patterns. Color and number in each cell represents the enrichment P-value (-log10 transformed, hypergeometric test p-value) of (SPE TF regulated) target DE proportions relative to the genome-wide proportion of DEGs for each GRN (row-wise) evaluated against a tissue/treatment condition in a natural variation dataset (column-wise). Only edges in the first bin (top 100k) of each network were taken.

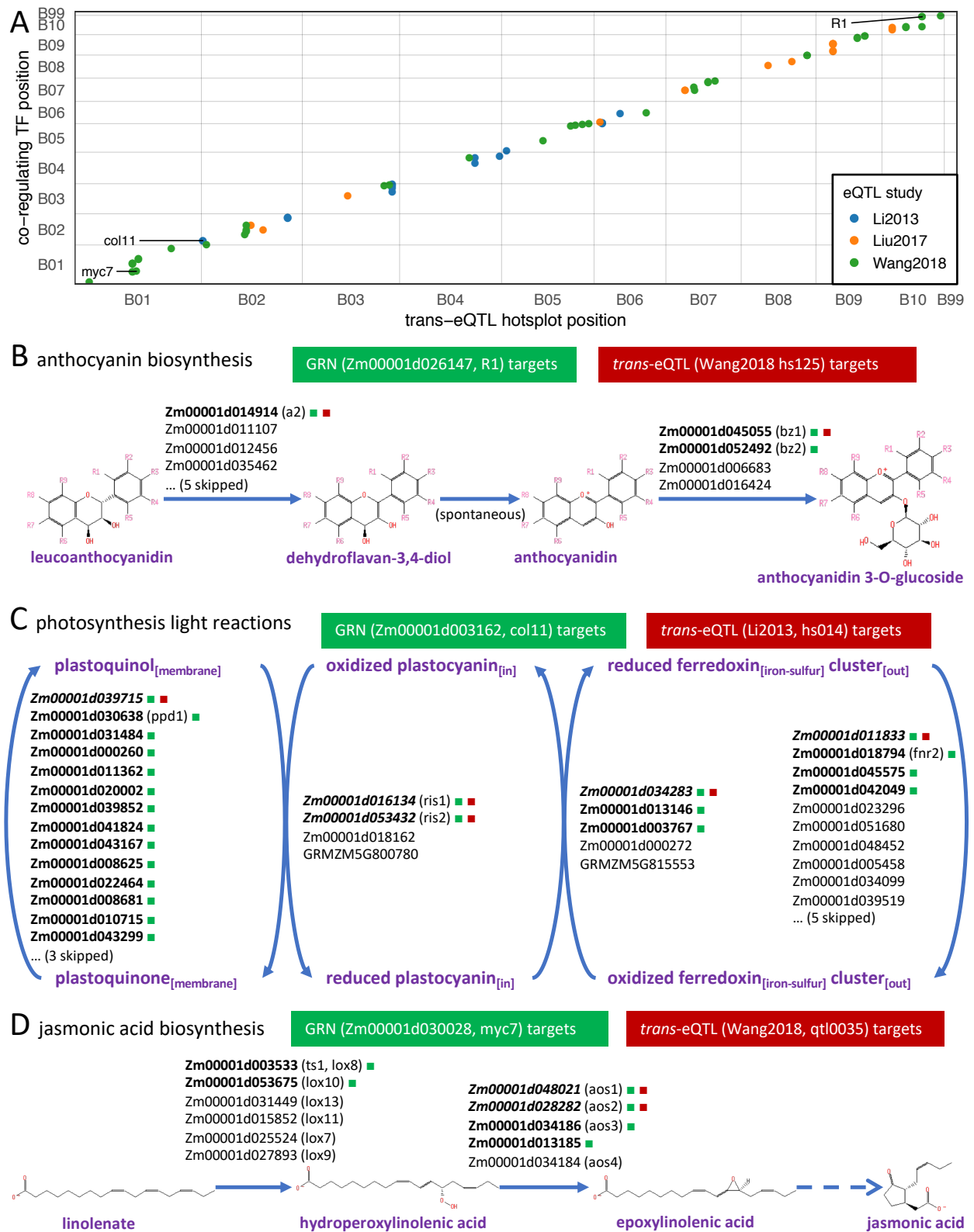


Figure 7. Identification of acting transcription factors underlying trans-eQTL hotspots identified in previous studies. (A) Co-localization of TFs predicted by GRNs in this study and trans-eQTL hotspots identified in previous studies that regulate the same set of targets. Each dot represents a TF supported by at least

two high quality networks to show significant co-regulation with at least one trans-eQTL hotspot, and are within 10-Mbp distance from the trans-eQTL hotspot location; (B)-(D) Identification of R1 (Zm00001d026147), col11 (Zm00001d003162) and myc7 (Zm00001d030028) co-localizing previous trans-eQTL hotspots and acting as the master regulator of maize anthocyanin biosynthesis pathway, photosynthesis light reaction pathway and jasmonic acid biosynthesis pathway, respectively.